ARTICLE

Synthesis, Characterization, and Carbon Dioxide Adsorption of Covalently Attached Polyethyleneimine-Functionalized Single-Wall Carbon Nanotubes

Eoghan P. Dillon, Christopher A. Crouse, and Andrew R. Barron*

Richard E. Smalley Institute for Nanoscale Science and Technology, Center for Biological and Environmental Nanotechnology, Carbon Nanotube Laboratory, and Department of Chemistry, Rice University, Houston, Texas 77005

ABSTRACT The reaction between fluorinated single-wall carbon nanotubes (F-SWNTs) and branched (M_w = 600, 1800, 10000, and 25000 Da) or linear (M_w = 25000 Da) polyethyleneimine (PEI) yields the covalent attachment of the polymer to the sidewalls of the nanotubes. The resulting PEI-functionalized SWNTs (PEI-SWNTs) were characterized by solid-state ^{13}C NMR, Raman spectroscopy, X-ray photoelectron spectroscopy, UV–vis spectroscopy, atomic force microscopy, transmission electron microscopy, and thermal gravimetric analysis studies. As expected, the number of polymer molecules per SWNT is larger for low molecular weight PEI than for high molecular weight PEI. However, above 1800 Da, the number of polymer molecules per SWNT does not vary as much. This is supported by Raman spectral data that shows the D:G ratio is relatively insensitive of the molecular weight for M_w > 1800 Da. The PEI-SWNTs are shown to have solubility in aqueous media of up to 0.4 mg · mL^{-1}. Solid-state ^{13}C NMR shows the presence of carboxylate substituents that have been attributed to carbamate formation as a consequence of the reversable CO_2 absorption to the primary amine substituents of the PEI. Desorption of CO_2 is accomplished by heating under argon at 75 °C, while the dependence of the quantity of CO_2 absorbed on temperature and the molecular weight of the PEI is reported. Under the conditions investigated the maximum absorption of 9.2% w/w is observed for PEI(25000)-SWNT at 27 °C. The possible CO_2 absorption applications of the PEI-SWNTs is discussed.

KEYWORDS: single-wall carbon nanotubes (SWNT) · polyethylenimine (PEI) · functionalization · carbon dioxide · absorption · polymer

The use of single-wall carbon nanotubes (SWNTs) for biological applications has been a prominent area of research over the last several years.[1–3] SWNTs have been proposed as candidates for numerous applications including biosensors[4] contrast agents for magnetic imaging,[5] tissue-growth scaffolds, [6] and drug delivery agents.[7] One major obstacle preventing the use of carbon nanotubes for widespread *in vivo* use is their lack of solubility in aqueous systems.[8] Due to their hydrophobic nature carbon nanotubes tend to aggregate together when exposed to most solvents, aqueous or organic. The physical adsorption of soluble polymers and/or surfactants, as well as the direct covalent sidewall functionalization of carbon nanotubes (CNTs) has provided useful methods to achieve dissolution in aqueous solvents allowing for their use in biological applications and the ability to interface CNTs with living cells.[1,8]

In this work we present the direct covalent attachment of a cationic polymer, polyethylenimine (PEI), to the sidewalls of SWNTs resulting in aqueous solubility. PEI, is a polyamine that exists in both a linear or branched form and is available in varying molecular weights. In its branched form (M_w ≥ 25000 Da) PEI has historically been used as a nonviral transfection agent for the delivery of plasmid DNA and nucleic acids into cells at physiological pH.[9,10] The loading of pDNA and nucleic acids results in electrostatic interactions between the positively charged protonated amines within the polymer and the anionic nucleic acid resulting in the formation of nanoparticles which are capable of being taken into the cell.[11] Recently the use of PEI as a successful transfection agent has also been expanded to include proteins and antibodies.[10]

Previous studies toward the use of PEI to promote the solubility and biological compatibility of CNTs have focused on the physical adsorption of PEI to multiwall carbon nanotubes[3] or through the formation of a PEI-SWNT copolymer with limited covalent attachment occurring through the formation of amide linkages exclusively at the open ends of SWNTs.[2] Margrave and coworkers demonstrated that the reaction of fluorinated-SWNTs (F-SWNTs) with primary

*Address correspondence to arb@rice.edu.

Received for review October 2, 2007 and accepted December 10, 2007.

Published online January 4, 2008.
10.1021/nn7002713 CCC: $40.75

amines allowed for the covalent sidewall functionalization of the nanotubes while maintaining the structural integrity of the original SWNT (Scheme 1).[12–14] We have previously adapted this methodology to allow for the formation of SWNT self-assembled monolayers[15,16] and the synthesis of amino acid substituted SWNTs with carboxylate termini.[17] While the amino acid derived SWNTs showed significant solubility over a wide pH range, we observed that aggregation occurred at high salt concentrations or in buffered solutions.[17] This effect limited their usefulness for cellular studies since significant intracellular aggregation was observed.[18]

We proposed to accomplish this through the direct covalent attachment of low molecular weight PEI ($M_w \leq 10000$ Da) along the sidewalls of SWNTs. The primary amines present in PEI should be capable of reaction with F-SWNTs (*cf.* Scheme 1). The presence of the primary and secondary amines also allows for protonation at physiological pH (7.35), and thus the cationic character of the polymer should promote the dissolution of the SWNTs. In addition, we have shown that carbon nanomaterials with cationic (as opposed to anionic) substituents show significant enhancement in transmembrane transport.[19] PEI was also chosen for its low cytotoxicity at low molecular weights, and the large number of primary and secondary amines available for covalent attachment to the sidewalls of the SWNTs.

RESULTS AND DISCUSSION

PEI-SWNTs were prepared by the reaction of F-SWNTs with the appropriate molecular weight PEI in EtOH suspension in the presence of a pyridine catalyst (see Experimental Section). PEI-SWNTs were prepared using branched PEI of M_w = 600, 1800, 10000, and 25000 Da and linear PEI (M_w = 25000 Da), yielding PEI(600)-SWNT, PEI(1800)-SWNT, PEI(10000)-SWNT, PEI(25000)-SWNT, and linear-PEI (M_w = 25000 Da), respectively.

Although the reaction of F-SWNTs with amines has been shown to result in covalent attachment by both

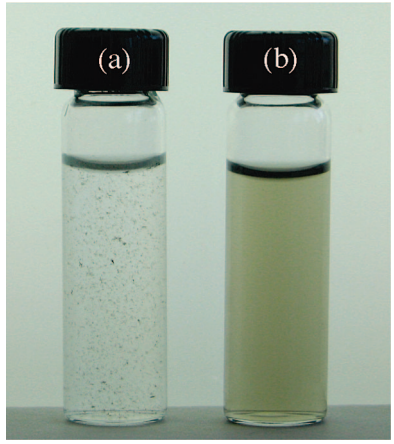

Figure 1. Comparison of (a) noncovalently attached PEI(600)-SWNT, and (b) covalently attached PEI(600)/SWNTs, after aqueous dialysis for 20 min and 4 days, respectively.

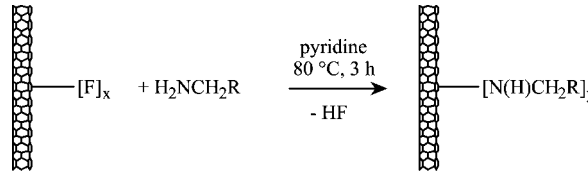

Scheme 1. Synthesis of Functionalized SWNTs from F-SWNTs

scanning tunneling microscopy and NMR measurements,[16,20] we have prepared the noncovalent conjugate using both pristine SWNTs and F-SWNTs and PEI (M_w = 600 Da) in order to further confirm the covalent attachment in PEI-SWNTs. The noncovalent conjugates, PEI(600)/SWNT and PEI(600)/F-SWNTs, are soluble in water upon preparation; however, aqueous dialysis for 20 min results in the aggregation and precipitation of the nanotubes. In contrast, each of the PEI-SWNTs prepared in the presence of a pyridine catalyst shows no alteration in solubility (miscibility) after 4 days of dialysis. The comparison between covalent and noncovalent attachment is shown in Figure 1.

The PEI-SWNTs were tested for aqueous solubility at neutral pH. For example, PEI(600)-SWNTs were sonicated for 15 min in deionized water and then were transferred to a centrifuge tube. The solution was centrifuged to ensure all of the bundled tubes and insoluble material were removed from the decant. The resulting decant was deep black in color with no visible particulates in the solution. The solubility was determined to 0.4 mg · mL^{-1}.[21] Each of the branched PEI-SWNTs showed comparable solubility at neutral pH suggesting that even at the lowest molecular weight the branched PEI imparts optimum solubilization of the

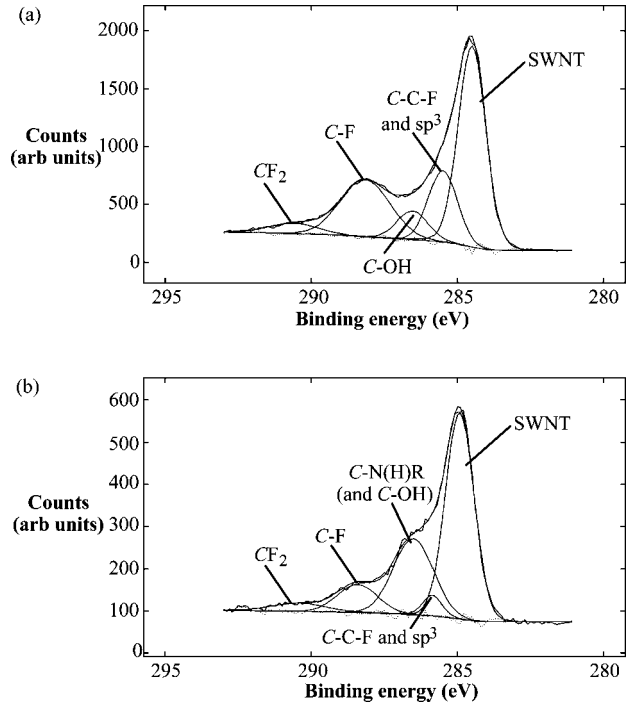

Figure 2. C_{1s} high-resolution XPS spectra for (a) F-SWNTs and (b) PEI(10000)-SWNTs. Peak fits and assignments are shown.

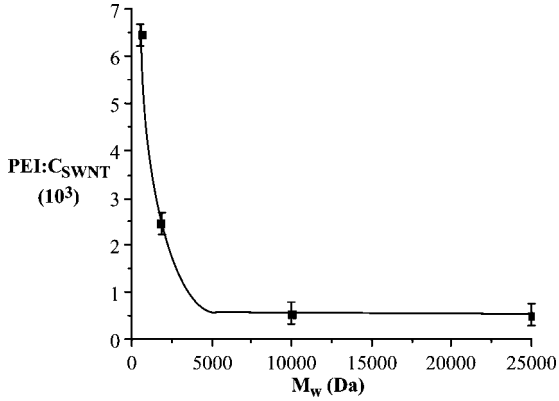

Figure 3. Plot of the number of PEI molecules per SWNT carbon (PEI:C_{SWNT}) as a function of the molecular weight (Da).

SWNT. In contrast, linear-PEI-SWNT shows only transient miscibility in water. After sonication a suspension is observed for only a few minutes before aggregation and precipitation occur. The branched PEI-SWNT's showed good solubility between pH 1.7 and 8.31. At any pH above these values aggregation was observed. However, the rate of aggregation is dependent on the source of basicity. Addition of NaOH solution resulted in aggregate over a period of about 6 h, whereas addition of $NaHCO_3$ solution resulted in instantaneous aggregation. This observation is consistent with the CO_2 absorbing qualities of the PEI-SWNT's (see below).

As expected, based upon the known reaction of F-SWNTs with amines, the X-ray photoelectron spectroscopy shows a decrease in the fluorine concentration for the PEI-SWNTs *versus* the F-SWNT starting material with a concomitant increase in the nitrogen content. However, whereas the reaction of F-SWNTs with simple amines results in a loss of the majority of fluorine, the C_{1s} spectrum shows that there remains significant fluorine concentration (Figure 1).[20] This is consistent with the attachment of each polymer via a limited number of amine groups, allowing the majority of the hydrophilic amine functional groups available to ensure solubility. This is rather than the polymer wrapping around the SWNT with extensive covalent attachment, leaving a more hydrophobic organic backbone, which would limit organic solubility. Another interesting observation is that the signal due to the CF_2 groups (290.62 eV) appears to be largely unaffected by the reaction of the amine (*cf.* Figure 2), while the peak assigned to the sidewall C−F groups (288.61 eV) is diminished in concert with the presence of the sidewall C−N substituents (286.35 eV). This observation suggesting that the reaction of F-SWNTs with amines occurs preferentially at the sidewall C−F groups rather than the defect CF_2 moieties.

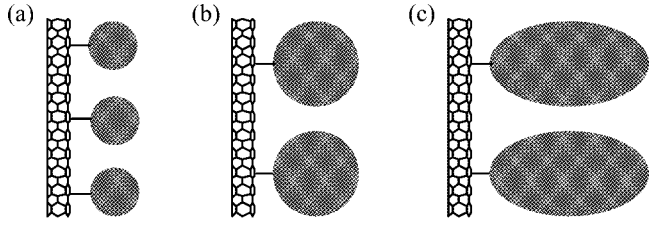

Figure 4. Schematic representation of PEI-SWNTs with molecular weights of (a) 600 Da, (b) 10000 Da, and (c) 25000 Da, showing the orientation of PEI substituents accounting for the insensitivity of number of polymers per SWNT as a function of M_w. This is in contrast to the expected decrease in PEI:C_{SWNT} that would be expected with increased N−C_{SWNT} attachments for higher M_w PEI.

TABLE 1. Selected Physical and Spectroscopic Data for Branched PEI-SWNTs

PEI M_w (Da)	PEI:C_{SWNT}	Raman D:G	CO_2 absorption at 75 °C (%)	CO_2 efficiency, mol of CO_2/mol of PEI
600	1:155	0.448	4.1	0.0217
1800	1:405	0.291	4.8	0.0827
10000	1:1910	0.273	5.2	0.143
25000	1:2065	0.273	7.2	0.159

The PEI:SWNT ratio can be determined from the thermogravimetric analysis (TGA); see Table 1.[17] TGA of as prepared PEI-SWNTs shows a mass loss between 25 and 75 °C, consistent with desorption of water (and possibly CO_2, see below), followed by the decomposition of the PEI substituents and the re-

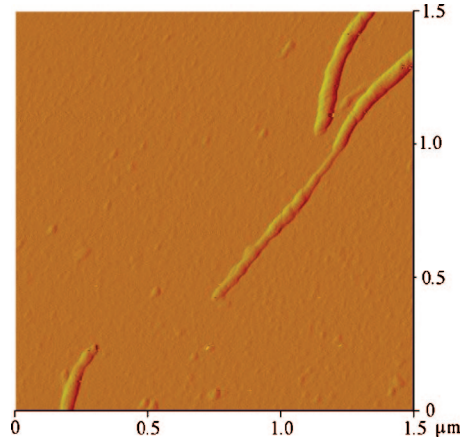

Figure 5. AFM image of a PEI(600)-SWNT showing the presence of PEI "globules" on the SWNT.

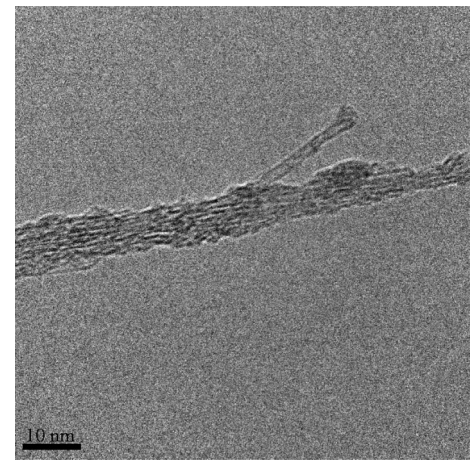

Figure 6. TEM image of a single PEI(600)-SWNTs exposed from a bundle.

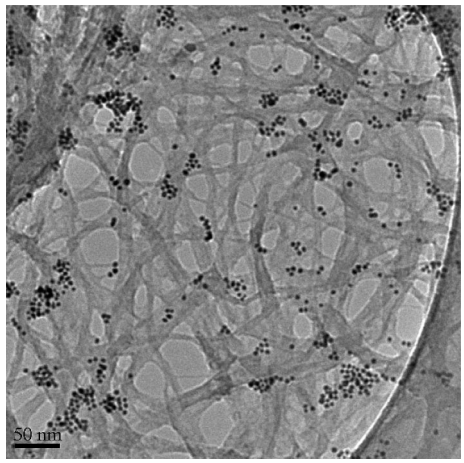

Figure 7. TEM image of PEI(600)-SWNTs functionalized with gold nanoparticles formed from the reduction of $HAuCl_4$ by the PEI substituents.

formation of the parent SWNT at 250 °C. As may be expected, the number of polymer molecules per SWNT is larger for low-molecular weight PEI (M_w = 600 Da) than for high-molecular weight PEI (M_w = 25000 Da). However, it is worth observing that above 10000 Da, the number of polymer molecules per SWNT remains essentially constant (Figure 3). It may be assumed that increasing the molecular weight of the PEI allows for more attachment points *via* the additional NH_2 groups, and as a consequence a smaller number of PEI molecules would be required to functionalize the entire SWNT. Instead, a large increase in the molecular weight (*i.e.*, 10000 *vs* 25000) does not correspond to a change in the number of PEI polymer molecules per SWNT. We propose that this is due to the hydrophilic PEI being repelled from the hydrophobic surface of the SWNT (Figure 4, panels a and b) rather than wrapping around the SWNT to make additional covalent attachments (Figure 4, panel c). The surface globular nature of the PEI substituents is confirmed by atomic force microscopy (AFM) and TEM, while the extent of functionalization is consistent with Raman spectroscopy.

Atomic force microscopy and TEM also confirmed the presence of PEI on the sidewalls of the tubes. Figure 5 shows PEI(10000)-SWNTs spin-coated on a freshly cleaved mica surface. The images are typical of substituted SWNTs, and analysis of the height data along the length of the nanotubes suggests that the majority of the tubes are coated with the polymer when compared to the height data of unfunctionalized tubes. Cross sectional analysis of the data in Figure 5 shows a height of 7–10 nm compared to 2–5 nm for a pristine SWNT.

Figure 6 displays a TEM image of a single PEI(600)-SWNT protruding from a bundle of tubes. Bundling of the tubes occurs when the sample is drop-cast onto the TEM grid and the water from which the sample is contained slowly evaporates causing concentration of the solution and subsequent aggregation and bundling of the tubes. Due to the organic nature of PEI it was difficult obtain images of the

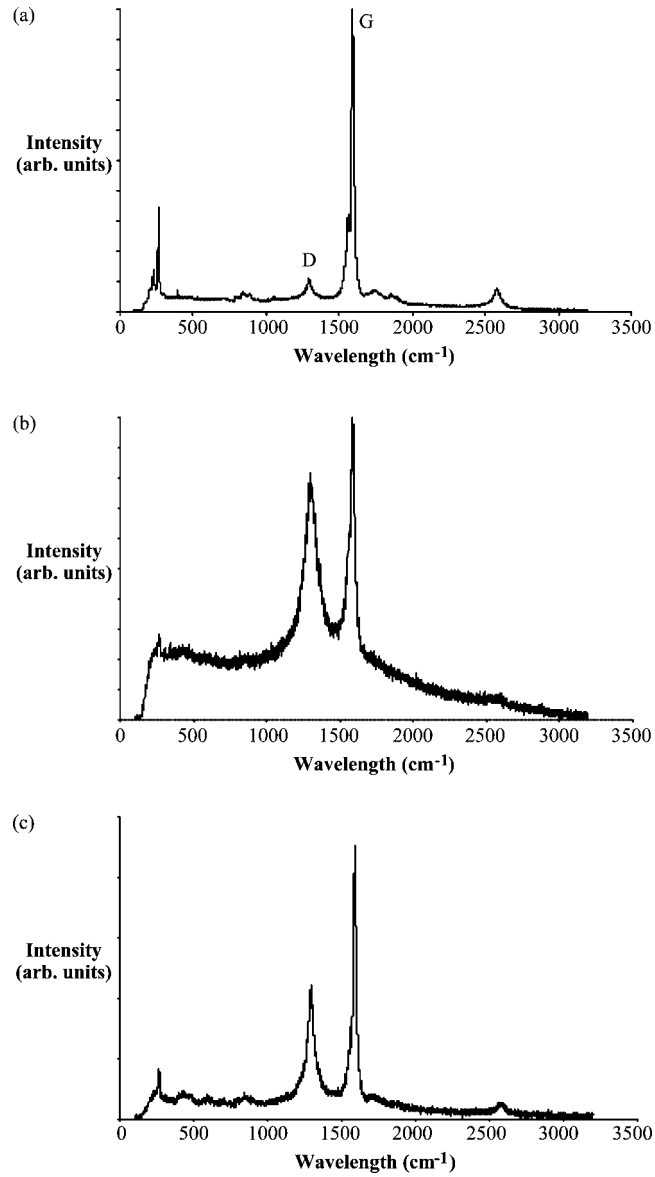

Figure 8. Raman spectrum (780 nm) of (a) purified SWNTs, (b) F-SWNTs, and (c) PEI(600)-SWNTs.

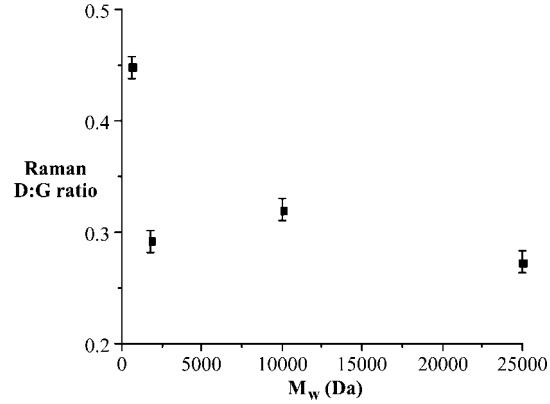

Figure 9. Plot of the Raman D:G ratio as a function of PEI molecular weight (Da) for PEI-SWNTs.

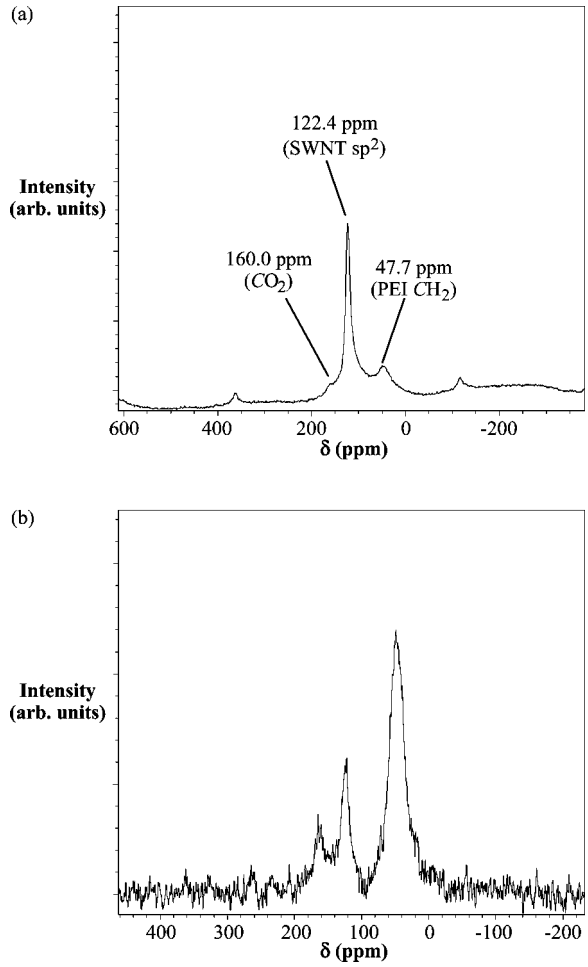

Figure 10. Solid-state NMR spectra of PEI(600)-SWNTs. (a) ^{13}C MAS NMR spectrum with a 12 kHz spinning speed, and (b) $^{1}H-^{13}C$ CPMAS spectrum with a 7 kHz spinning speed.

polymer on the SWNTs with TEM as it would combust when exposed to the electron beam. It has been previously reported that linear-PEI can be used as a reducing agent in the formation of gold nanoparticles from $HAuCl_4$.[22] Extending this prior work with linear-PEI, the presence of branched-PEI on the SWNTs was indirectly confirmed by the addition of $HAuCl_4$ to the PEI-SWNT solution and heating the solution for 20 min at 70 °C. Upon completion of heating, the samples were allowed to cool and where drop-cast onto TEM grids and reimaged. The presence of gold nanoparticles along the sidewalls of tubes (Figure 7) and not in the void space demonstrates the presence of PEI on the sidewalls of the SWNTs.

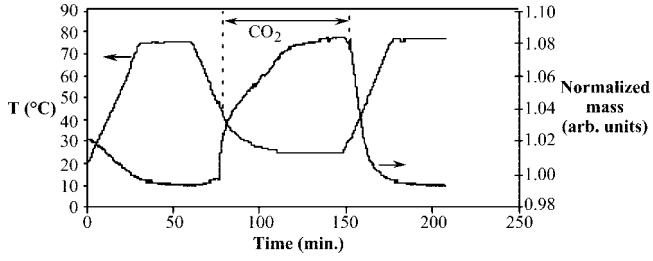

Figure 11. TGA of PEI(25000)-SWNT showing the mass change associated with the adsorption and desorption of CO_2. The mass has been normalized to the lowest mass recorded, which is equivalent to PEI(25000)-SWNT.

The Raman spectrum, obtained with a 780 nm excitation laser, for the purified HiPco SWNTs (Figure 8a) displayed a strong tangential G mode at 1592 cm^{-1} accompanied by a small peak at 1292 cm^{-1}, corresponding to the D (disorder) mode due to sp^3-hybridized carbons, suggesting a low degree of defect sites within the continuous graphitic sheet of the nanotubes.[23] The presence of prominent radial breathing modes appearing at 233 and 267 cm^{-1} suggests that the nanotubes are truly single walls.[24] Fluorination of the purified SWNTs resulted in a substantial increase in the number of sp^3-hybridized carbons with a concomitant increase in the D mode and a decrease in the tangential G mode associated with sp^2-hybridized carbons from the graphitic sidewalls (Figure 8, panel b). This increase in the ratio of the sp^3:sp^2 ratio is described by the D:G ratio. An increase in the D:G ratio is also accompanied by an almost complete loss of the radial breathing modes, suggesting that the continuous delocalization of electrons throughout the nanotubes has been highly disrupted due to covalent attachment of the fluorine atoms to the nanotubes.[12] As was observed in the covalent addition of diamines to the sidewalls of F-SWNTs[13] the structural integrity of the original purified nanotubes is partially re-established by the addition of PEI to the F-SWNTs under the reaction conditions previously described. The sp^3/sp^2 ratio mode present in the PEI-SWNT spectra (*e.g.*, Figure 8, panel c) is substantially lower than that observed for the F-SWNTs, however, higher than the observed ratio for purified SWNTs without functionalization. This result, accompanied by an increase in the nitrogen content of the sample and a decrease in the fluorine content as confirmed through X-ray photoelectron spectroscopy (XPS), suggests that the PEI has been covalently attached to the sidewalls resulting in the displacement of the fluorine atoms. The presence of radial breathing modes and an increase in the tangential mode suggest that portions of the original graphitic sidewall have been re-established during the reaction process.

If our model for the morphology of the PEI substituents as a function of molecular weight is correct, then the number of "attachment" points (*i.e.*, the number of sp^3 carbons per SWNT) should follow the same trend as the number of PEI molecules per SWNT carbon. As may be seen from Figure 9, the number of sidewall sp^3 carbons is greater (*i.e.*, large D:G ratio) for PEI with a M_w = 600 Da, than those with higher molecular weights. However, there appears to be no significant variation in the D:G ratio for PEI above M_w = 1800 Da (Figure 9). This is consistent with our model shown in Figure 4.

The UV–vis−NIR and fluorescence spectra obtained for the PEI-SWNTs assists in confirming the covalent functionalization of the SWNTs through the loss in the van Hove absorbance and fluorescence as compared to unfunctionalized SWNTs, respectively. Both are due to the partial disruption in the delocalized electronic structure of the SWNTs due to the sp^3-hybridized carbons present in the sidewall at the sites of covalent attachment to the PEI.[13]

We have previously been able to assign the sp^3 carbon on the SWNT sidewall for a range of functionalized SWNTs.[20] However, in the present case with the low number of PEI molecules per SWNT and the consequently lower number of SWNT sp^3 carbons we were unable to conclusively observe the SWNT sp^3 carbon. The direct pulse ^{13}C MAS NMR spectrum of a sample of PEI(600)-SWNTs (Figure 10, panel a) shows three signals that can be assigned to the sidewall sp^2 carbon ($\delta = 122.4$), the aliphatic CH_2 groups of the PEI ($\delta = 47.7$), and a small shoulder at ~160 ppm consistent with a carbonyl group. The $^1H-^{13}C$ CPMAS spectrum (Figure 10, panel b) suppresses the SWNT sp^2 signal and allows for the clearer observation of the carbonyl ($\delta = 160.0$). The presence of the carbonyl signal was originally assumed as being due to residual carboxylate groups on the SWNT; however, several observations suggested otherwise. First, the relative intensity of the peak in comparison with the PEI aliphatic signal suggested a much higher concentration than would be expected. Second, the carbonyl content appeared to be dependent on the age of the sample. Third, the sensitivity to bicarbonate (as compared to hydroxide) suggested a reaction with CO_2. Lastly, PEI is known to react with CO_2 by means of the amines to form a carbamate (eq 1).[25]

$$R-NH_2 + CO_2 \rightarrow R-N(H)CO_2^- + H^+ \qquad (1)$$

CO_2 Absorption. The potential absorption of carbon dioxide by the PEI-SWNTs was investigated by TGA. As discussed above, heating samples to 75 °C under argon results in an initial decrease in mass due the presence of moisture (and what is apparently ambient CO_2 absorption) in the sample. Once a constant mass was achieved, the flow gas was switched to CO_2 and the temperature reduced to a set level. As can be seen from Figure 11, once CO_2 is introduced the mass increases significantly until a stable maximum. Once the carrier gas is switched back to argon, a mass loss occurs back to the original mass for the PEI-SWNT. As is shown in Table 1, for a particular experimental temperature the percentage increase in mass is dependent on the molecular weight of the PEI (in the PEI-SWNT).

The ability of the PEI-SWNT to absorb CO_2 should be related to the number and availability of NH_2 groups for reaction. Since the percentage PEI in each PEI-SWNT is known, the efficiency of adsorption at a particular temperature can be calculated, *i.e.*, the mass of CO_2 per mass of PEI. Assuming an average molecular weight of each polymer, then a molar efficiency can be estimated that provides an indication of the number of CO_2 molecules adsorbed per polymer unit. Figure 12 shows a plot of efficiency as a function of molecular weight of the PEI.

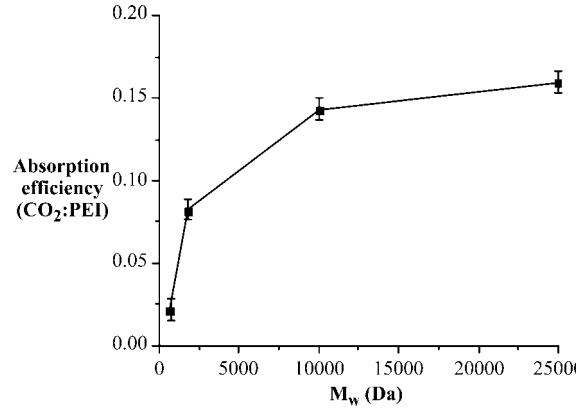

Figure 12. A plot of CO_2 adsorption efficiency as a function of molecular weight of the PEI for PEI-SWNTs.

The ability to reversably adsorb CO_2 is an important property for any CO_2 sequestration system. In order to determine the stability of the PEI-SWNTs to adsorption/desorption and thermal cycling, samples were repeatedly heated to 75 °C under argon and then cooled to ambient under CO_2. In each case the final mass for both PEI-SWNT and CO_2-PEI-SWNT is within 2% of the previous value showing the stability of the PEI-SWNTs. Furthermore, when the PEI-SWNTs were exposed to CO_2 for extended periods (at a constant temperature), there is no further increase in adsorption (*e.g.*, Figure 13).

In the above experiments the PEI-SWNT was exposed to 1 atm of CO_2 at 75 °C; however, the equilibrium absorption is dependent on the temperature. Figure 14 shows the TGA for PEI(10000)-SWNT heated to 110 °C under argon, followed by exposure to CO_2 at a range of temperatures between 75 and 25 °C. Clearly as the temperature is decreased the mass reached a new equilibrium. A plot of equilibrium CO_2 adsorption *versus* temperature is given in Figure 15. On the basis of the data in Figure 15, it can be determined that for

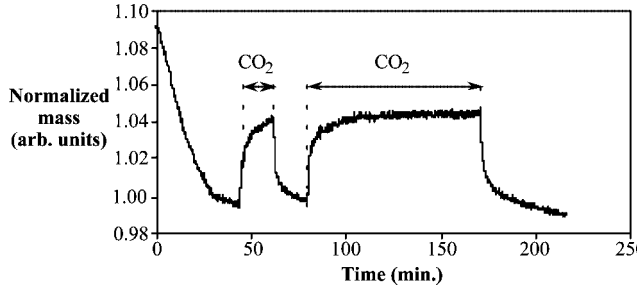

Figure 13. TGA of PEI(600)-SWNT showing the mass change associated with the repeated adsorption and desorption of CO_2 irrespective of exposure times. The mass has been normalized to the lowest mass recorded, which is equivalent to PEI(600)-SWNT.

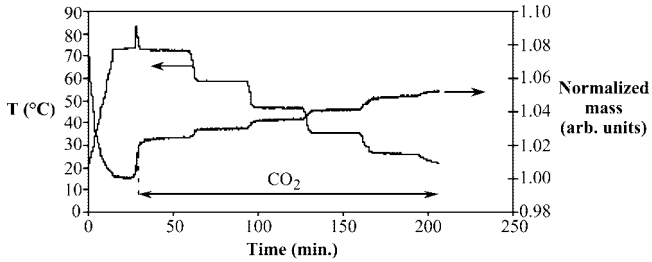

Figure 14. TGA for PEI(10000)-SWNT heated to 110 °C under argon, followed by exposure to CO_2 at a range of temperatures showing the increase in CO_2 adsorption with decrease in temperature.

PEI(10000)-SWNTs complete dissociation of CO_2 occurs at 115 °C even under a CO_2 atmosphere. Investigation of the temperature dependence of the other M_w PEI-SWNTs suggest that the zero point temperature (i.e., the temperature at which no CO_2 is absorbed) is essentially constant but that as shown above the absolute efficiency is dependent on the M_w.

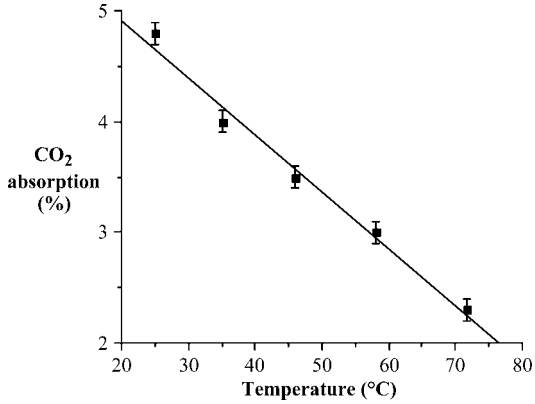

Figure 15. A plot of CO_2 adsorption efficiency as a function of temperature for PEI(10000)-SWNT.

CONCLUSIONS

We report the covalent attachment of branched PEI to the sidewalls of SWNTs through the use of F-SWNT precursors. The structural integrity of the original purified SWNT is maintained upon covalent functionalization with PEI, and solubility of the SWNTs in aqueous media is achieved. The PEI-SWNTs are readily dispersed in both aqueous and phosphate buffer solution. In this regard, the PEI-SWNTs offer potential applications with respect to biological applications.

Branched-PEI ($M_w > 25000$ Da) is necessary to observe transfection of DNA plasmids across a cell membrane.[9] It is our hope that tethering low molecular weight PEI (M_w 600–10000) onto a SWNT would achieve the same results due to the increased molecular weight of the system and cationic character across the surface of the tube, yet would exhibit the lower toxicity associated with the low M_w PEIs. The PEI-SWNTs prepared herein exhibit no cytotoxicity toward human embryonic kidney epithelial cells;[19] however, the length of the SWNTs employed meant that they were not capable of crossing cell membranes. Work is ongoing to reproduce this work with cut nanotubes to improve the cellular uptake of the PEI-SWNTs.

The reversible absorption of CO_2 is of importance in a number of applications. Although the use of SWNTs for large-scale CO_2 sequestration is impractical, the absorption in closed systems such as spacecraft and orbiting space stations as well as submarines is where a lightweight reusable adsorption system offers a potential solution. We are presently investigating the conditions under which Bucky-paper of the PEI-SWNTs provide optimum absorption and low-energy desorption of CO_2 from ambient atmospheres.

EXPERIMENTAL SECTION

Pristine HiPco SWNTs were obtained through the Carbon Nanotube Laboratory (CNL) at Rice University and were purified by the wet-air oxidation procedure at 250 °C for 24 h to remove any iron and carbon impurities.[26] The degree of purification was determined using TGA analysis in air and showed that the purified SWNTs contained less than 3% iron content after purification. Fluorination of the purified nanotubes was achieved using a previously reported procedure and yielded a stoichiometry of $C_{2.7}F$ as determined by the difference in mass and was confirmed XPS analysis. Branched polyethyleneimine (M_w = 600, 1800, 10000, and 25000 Da) and linear polyethyleneimine (M_w 25000 Da) (Alfa Aesar), EtOH (AAPER Alcohol), and pyridine (Aldrich) were used as received. All water was ultrapure (UP), obtained from a Millipore Milli-Q UV water filtration system.

Characterization was performed using a FEI XL30 Schottky field-emission environmental scanning electron microscope ESEM with EDAX energy dispersive spectroscopy capability and a JEOL 6500F thermal field-emission scanning electron microscope. These were used at accelerating voltages of 30 and 15 kV, respectively. Samples were mounted with carbon tape onto aluminum microscopy specimen mounts (Electron Microscopy Sciences). Before imaging, insulating samples were sputter coated (Plasma Sciences CRC 100 sputter coater) with a thin layer of gold or chromium to prevent charging. XPS were acquired on a PHI 5700 ESCA system (Physical Electronics) at 15 kV, using an aluminum target and an 800 μm aperture. Samples were pressed into indium metal. Transmission electron microscopy was performed with a JEOL 2010 instrument at 100 kV utilizing a JEOL FasTEM system. Samples were dropped onto Cu grids with lacey carbon film (Electron Microscopy Sciences) and allowed to dry thoroughly before imaging. Raman spectroscopy on solids (both 785 and 532 nm excitation) was performed using a Renishaw Raman microscope. Samples were mounted on double-sided tape. Attenuated total reflectance infrared spectroscopy (ATR-IR, 4000–600 cm^{-1}) of solids was obtained using a Nicolet Nexus 670 FT-IR with a diamond window. UV/vis spectra (200–1400 nm) were collected using a Cary 5000 UV/vis−NIR spectrometer using quartz cuvettes. Thermal analysis was performed on a Seiko TG/DTA 200 using aluminum pans.

PEI-SWNT. Covalent functionalization of SWNTs was achieved through the reaction of branched and linear PEI with F-SWNTs by dispersing F-SWNTs (20 mg) in EtOH (25 mL) by the use of probe sonication for 20 min. This was combined with 25 mL of a 0.1 M branched-PEI (M_w 600) solution in EtOH into a 100 mL round-bottomed flask fitted with a condenser and a magnetic stir bar. Pyridine (1 mL) was added to the reaction mixture, and the reaction was brought to reflux, ~24 h, with continuous stirring. Upon completion of the reaction, SWNT recovery was achieved by filtration of the reaction mixture through a 0.2 μm membrane PTFE filter (Cole Parmer). The filtrate was washed with

copious amounts of absolute EtOH followed by deionized water to remove pyridine and any unreacted polymer. The PEI(600)-SWNT product was then removed from the filter paper without drying and transferred to a plastic centrifuge tube and was dispersed in deionized water *via* probe sonication, ~15 min. The suspended PEI-SWNTs were then centrifuged at 4400 rpm for 15 min. The PEI-SWNT decant was removed and stored at room temperature in a plastic centrifuge tube.

This same procedure was also repeated for the preparation of PEI(1800)-SWNT and PEI(10000)-SWNT using 0.04 and 0.008 M solutions of branched-PEI (M_w = 1800 and 10000 Da) in EtOH, respectively. The linear-PEI(25000)-SWNT was prepared using the above procedure with 25 mL of 0.003 M linear-PEI (M_w = 25000 Da) in EtOH.

PEI(600)/SWNT. Physical adsorption of PEI to the sidewalls of SWNTs was achieved by dispersing purified SWNTs (20 mg) into EtOH (25 mL) by probe sonication for 20 min. This was combined with 25 mL of a 0.1 M PEI (M_w = 600 Da) solution in EtOH in a 100 mL round-bottomed flask fitted with a condenser and a magnetic stir bar. The reaction mixture was brought to reflux, ~24 h, with continuous stirring. Upon completion, the recovery, purification, and storage of the PEI-adsorbed SWNT were achieved using the method previously described for the covalently attached PEI-SWNTs. A similar reaction is used to prepare PEI(600)/F-SWNT physical absorbed conjugates.

pH Solubility Studies. Solutions of pH 1.7, 3.25, 5.7, 8.31, 11.21, and 13.28 were prepared. Deionized water with a measured pH of 5.7 was also used for all samples. The acidic solutions (pH 1.7 and 3.25) were prepared by the dilution of 1 M HCl with water. The pH of each solution was constantly monitored using a pH probe. Two sets of basic pH solutions (pH 11.21 and 13.28) were prepared by the addition of dilution of $NaHCO_3$ and NaOH, respectively. An aqueous solution containing the PEI-SWNTs (2 mL of 4 mg · mL^{-1}) was then added to each solution.

CO_2 Absorption. CO_2 absorption experiments were carried out on a Seiko TG/DTA 200. The general procedure for the absorption experiments is shown below. PEI-functionalized SWNTs (5–10 mg) were loaded into an aluminum TGA pan and placed on the balance arm of the TGA. The chamber was sealed and purged with a steady flow of argon. The temperature of the system was ramped from room temperature to 110 °C at a rate of 3 °C · min^{-1}, in order to degas and dehydrate the sample. After the mass decrease stabilized to a constant mass, the gas in the system was changed to CO_2. Upon the change of gases, an immediate increase in weight was observed indicating that the PEI-SWNT's are absorbing the CO_2. The CO_2 flow was continued until constant weight was attained. In order to determine the effects of sample temperature, the sample temperature was adjusted to the desired measurement temperature after a constant weight had been reached.

Acknowledgment. Financial support for this work is provided by the Robert A. Welch Foundation and the National Science Foundation (Grant Number EEC-0647452, CBEN). Funds toward the purchase of the 200 and 500 MHz NMR spectrometers were provided by the Office of Naval Research and the National Science Foundation, respectively. The assistance of Dr. Lawrence B. Alemany with solid-state ^{13}C NMR measurements is gratefully acknowledged. F-SWNTs were provided by Jeyarama Ananta.

Supporting Information Available: SEM and AFM images, Raman, XPS, UV–visible spectra, and TGA of the PEI-SWNTs. This material is available free of charge *via* the Internet at http://pubs.acs.org.

REFERENCES AND NOTES

1. Chen, X.; Tam, U. C.; Czlapinksi, J. L.; Lee, G. S.; Rabuka, D.; Zettl, A.; Bertozzi, C. R. Interfacing carbon nanotubes with living cells. *J. Am. Chem. Soc.* **2006**, *128*, 6292–6293.
2. Hu, H.; Ni, Y.; Mandal, S. K.; Montana, V.; Zhao, B.; Haddon, R. C.; Parpura, V. Polyethyleneimine functionalized single-walled carbon nanotubes as a substrate for neuronal growth. *J. Phys. Chem. B* **2005**, *109*, 4285–4289.
3. Murugesan, S.; Park, T.; Yang, H.; Mousa, S.; Linhardt, R. J. Blood compatible carbon nanotubes - nano-based neoproteoglycans. *Langmuir* **2006**, *22*, 3461–3463.
4. Gooding, J. J. Nanostructuring electrodes with carbon nanotubes: a review on electrochemistry and applications for sensing. *Electrochim. Acta* **2005**, *50*, 3049–3060.
5. Sitharaman, B.; Kissell, K. R.; Hartman, K. B.; Tran, L. A.; Baikalov, A.; Rusakova, I.; Sun, Y.; Khant, H. A.; Ludtke, S. J.; Chiu, W.; Laus, S.; Toth, E.; Helm, L.; Merbach, A. E.; Wilson, L. J. Supermagnetic gadonanotubes are high-performance MRI contrast agents. *Chem. Commun.* **2005**, 3915–3917.
6. Harrison, B. S.; Atala, A. Carbon nanotube applications for tissue engineering. *Biomaterials* **2007**, *28*, 344–353.
7. Malmsten, M. Soft drug delivery systems. *Soft Matter* **2006**, *2*, 760–769.
8. Ramesh, S.; Ericson, L. M.; Davis, V. A.; Saini, R. K.; Kittrell, C.; Pasquali, M.; Billups, W. E.; Adams, W. W.; Hauge, R. H.; Smalley, R. E. Dissoultion of pristine single walled carbon nanotubes in superacids by direct protonation. *J. Phys. Chem. B* **2004**, *108*, 8794–8798.
9. Alexis, F.; Lo, S.; Wang, S. Covalent attachment of low molecular weight polyethyleneimine improves Tat peptide mediated gene delivery. *Adv. Mater.* **2006**, *18*, 2174–2178.
10. Didenko, V. V.; Ngo, H.; Baskin, D. S. Polyethyleneimine as a transmembrane carrier of fluorescently labeled proteins and antibodies. *Anal. Biochem.* **2005**, *344*, 168–173.
11. Kim, M. S.; Diamond, S. L. Controled release of DNA/polyamine complex by photoirradiation of a solid phase presenting O-nitrobenzyl ether tethered spermine or polyethyleneimine. *Bioorg. Med. Chem. Lett.* **2006**, *16*, 5572–5575.
12. Mickelson, E. T.; Huffman, C. B.; Rinzler, A. G.; Smalley, R. E.; Hauge, R. H.; Margrave, J. L. Fluorination of single-wall carbon nanotubes. *Chem. Phys. Lett.* **1998**, *296*, 188–194.
13. Stevens, J. L.; Huang, A. Y.; Peng, H.; Chiang, I. W.; Khabashesku, V. N.; Margrave, J. L. Sidewall amino functionalization of single-walled carbon nanotubes through fluorination and subsequent reactions with terminal diamines. *Nano Lett.* **2003**, *3*, 331–336.
14. Saini, R. K.; Chiang, I. W.; Peng, H.; Smalley, R. E.; Billups, W. E.; Hauge, R. H.; Margrave, J. L. Covalent sidewall functionalization of single wall carbon nanotubes. *J. Am. Chem. Soc.* **2003**, *125*, 3617–3621.
15. Zeng, L.; Pattyn, N.; Barron, A. R. Attachment of functionalized single-walled carbon nanotubes (SWNTs) to silicon surfaces. Submitted for publication.
16. Zhang, L.; Zhang, J.; Schmandt, N.; Cratty, J.; Khabashesku, V. N.; Kelly, K. F.; Barron, A. R. AFM and STM characterization of thiol and thiophene functionalized SWNT's: pitfalls in the use of chemical markers to determine the extent of sidewall functionalization in SWNT's. *Chem. Commun.* **2005**, 5429–5431.
17. Zeng, L.; Zhang, L.; Barron, A. R. Tailoring aqueous solubility of functionalized single-wall carbon nanotubes over a wide pH range through substituent chain length. *Nano Lett.* **2005**, *5*, 2001–2004.
18. Zhang, L.; Zeng, L.; Barron, A. R.; Monteiro-Riviere, N. A. Biological interactions of functionalized single-wall carbon nanotubes in human epidermal keratinocytes. *Int. J. Toxicol.* **2007**, *26*, 103–113.
19. Yang, J.; Wang, K.; Driver, J.; Yang, J.; Barron, A. R. The use of fullerene substituted phenylalanine amino acid as a passport for peptides through cell membranes. *Org. Biomol. Chem.* **2007**, *5*, 260–266.
20. Zeng, L.; Alemany, L. B.; Edwards, C. L.; Barron, A. R. Demonstration of covalent sidewall functionalization of single wall carbon nanotubes by NMR spectroscopy: side chain length dependence on the observation of the sidewall sp^3 carbons. Submitted for publication.
21. Moore, V. C.; Strano, M. S.; Haroz, E. H.; Hauge, R. H.; Smalley, R. E. Individually suspended single-walled carbon nanotubes in various surfactants. *Nano Lett.* **2003**, *3*, 1379–1382.

22. Hu, X.; Wang, T.; Qu, X.; Dong, S. In-situ synthesis and characterization of multiwalled carbon nanotube/Au nanoparticle composite materials. *J. Phys. Chem. B* **2006**, *110*, 853–857.
23. Dresselhaus. M. S. Pimenta. M. A. Ecklund. P. C. Dresselhaus. G. *Raman Scattering in Materials Science*.ed. Webber, W. H. , Merlin, R. , Eds.; Springer-Verlag:Berlin, 2000.
24. Saito, R.; Dresselhaus, G. ; Dresselhaus, M. S. *Physical Properties of Carbon Nanotubes*; Imperial College Press: London, England, 1998.
25. (a) Khatri, R. A.; Chuang, S. S. C.; Soong, Y.; Gray, M. Thermal and chemical stability of regenerable solid amine sorbent for CO_2 capture. *Energy Fuels* **2006**, *20*, 1514–1520. (b) Rolker, J.; Seiler, M.; Mokrushina, L.; Arlt, W. Potential of branched polymers in the field of gas absorption: experimental gas solubilities and modeling. *Ind. Eng. Chem. Res.* **2007**, *46*, 6572–6583.
26. Chiang, I. W.; Brinson, B. E.; Huang, A. Y.; Willis, P. A.; Bronikowski, M. J.; Margrave, J. L.; Smalley, R. E.; Hauge, R. H. Purification and characterization of single-wall carbon nanotubes (SWNTs) obtained from the gas-phase decomposition of CO (HiPco Process). *J. Phys. Chem. B* **2001**, *105*, 8297–8301.